

## Research Article

# Nuclear localization of mouse fibroblast growth factor 2 requires N-terminal and C-terminal sequences

A. Foletti, F. Vuadens and F. Beermann\*

ISREC (Swiss Institute for Experimental Cancer Research), NCCR Molecular Oncology, Chemin des Boveresses 155, 1066 Epalinges s/Lausanne (Switzerland), Fax: +41 21 6526933, e-mail: [friedrich.beermann@isrec.unil.ch](mailto:friedrich.beermann@isrec.unil.ch)

Received 1 July 2003; accepted 14 August 2003

**Abstract.** In vertebrates, different isoforms of fibroblast growth factor 2 (FGF2) exist, which differ by their N-terminal extension. They show different localization and expression levels and exert distinct biological effects. Nevertheless, genetic inactivation of all FGF2 isoforms in the mouse results in only mild phenotypes. Here, we analyzed mouse FGF2, and show that, as in the human, mouse FGF2 contains CTG-initiated high molecular-weight (HMW) isoforms, which contain a nuclear localization signal, and which mediate localization of this isoform to the nucleus. Using green fluorescent protein-FGF2 fusions, we furthermore observed, that C-terminal

deletions disable nuclear localization of the short low-molecular-weight (LMW) 18-kDa isoform. This loss of specific localization is accompanied by a loss in heparin binding. We therefore suggest that, first, localization of mouse FGF2 is comparable to that in other vertebrates and, second, FGF2 contains at least two sequences important for nuclear localization, a nuclear localization sequence at the N terminus which is only contained in the HMW isoform, and another sequence at the C terminus, which is only required for localization of the LMW 18-kDa isoform.

**Key words.** bFGF; GFP; nuclear localization; FGF2; mouse; transfection; knockout.

Basic fibroblast growth factor (FGF2; heparin-binding growth factor 2) is the prototype of the FGF family, and was first isolated from bovine pituitary gland and from brain. Since then, identification of FGF family members has continued and, currently, at least 23 distinct members have been identified in mammals. Members of the FGF family demonstrate a variety of properties, depending on cell type and context. FGFs induce cell-to-cell signaling by interacting with high-affinity cell surface receptors. Four receptor genes have been identified that encode high-affinity receptors, and the number of receptor species is extended by alternative splicing which changes the ligand affinity of some receptors. Additionally, on the cell surface, FGF2 interacts with heparan sulfate proteo-

glycans (HSPGs) whose function may be the stabilization of the FGF2-FGFR complex [1].

An unusual feature of FGF2 is the use of alternative CUG initiation codons to generate isoforms extended at the amino terminus. For human FGF2, five isoforms have been described; four high-molecular-weight (HMW) forms where translation starts at four different CUGs, and one low-molecular-weight (LMW) form where translation starts at the common translation start site [2–4]. Studies on the localization of FGF2 showed that the HMW forms localized exclusively to the nucleus and nucleolus [5–7]. The N-terminal region of the HMW forms was shown to contain a nuclear localization signal and to be able to lead fusion proteins to the nucleus [6, 8]. The correct distribution of the HMW isoforms depends on the methylation of three arginine residues present in the N terminus [9–11].

\* Corresponding author.

In contrast to the HMW forms, mechanisms controlling localization and the trafficking pathway of the 18-kDa isoform are still a matter of debate. The 18-kDa isoform does not contain any known secretory signal sequence, and secretion from cells uses an alternative pathway which is independent of the endoplasmic reticulum (ER)-Golgi complex [12] and is energy dependent [13]. The secreted FGF2 proteins can act in an autocrine and paracrine mode stimulating cell proliferation or migration [14]. FGF2 has been shown to accumulate in the nucleus and to bind to nuclear chromatin when administered exogenously [7, 15–19]. Moreover, the exogenous 18-kDa isoform provided to endothelial cells enters the nucleus specifically in the G1 phase of the cell cycle [15, 16]. This may include internalization of FGF2 and translocation to the nucleus together with the receptor [20–22]. Even intracrine FGF2 may enter the nucleus complexed with truncated forms of FGFR-1 and FGFR-2 devoid of the transmembrane region [23].

The relative amounts of individual forms of FGF2 vary among cell types and tissues during development and adulthood [24–27]. In vivo studies, using transgenic mice, showed that translation was regulated in a tissue-specific manner [28]. A cytokine-specific induction of HMW isoforms was observed in rat astrocytes [29] and a direct correlation exists between HMW isoform expression and stress conditions such as heat shock and oxidative stress in normal cells [27]. When expressed in NIH3T3 cells, HMW forms but not the LMW form allowed growth under low-serum conditions and in soft agar [14]. The LMW form, forced to enter the nucleus by fusion to the nuclear localization signal (NLS), was able to mimic the effects of HMW forms inducing cells to grow in low serum. These results point again to a specific function of the protein depending on the localization [11]. Nevertheless, overexpression of either 18-kDa or HMW FGF2 isoforms promotes cell transformation in a dose-dependent manner [30] and upregulation of all FGF2 isoforms was shown to be a critical component in melanoma progression [31].

Genetic experiments addressing FGF2 function in mammals have been performed in the mouse. Gene inactivation of mouse FGF2 revealed a mild phenotype, including neuronal defects, decreased bone mass, delayed wound healing and dilated cardiomyopathy [32–39]. In our experiments, the gene-targeting experiment did not remove the complete coding sequence of mouse FGF2, but only those encoding amino acids C-terminal from amino acid 81, resulting in an FGF2-lacZ fusion protein [38]. Nevertheless, removal of this stretch of the protein was sufficient to abolish FGF2 function [38, 39]. Since intracellular localization has not been reported for mouse FGF2, we have addressed this issue to potentially enable or improve studies in transgenic experiments. In addition, we set out to define areas of both long and short isoforms implicated in

nuclear or cytoplasmic localization, using N- and C-terminal fusions of mouse FGF2 to green fluorescence protein (GFP). Our results reveal the existence of a potential second nuclear localization sequence at the C terminus which is only needed for the LMW 18-kDa isoform.

## Materials and methods

### Analysis of genomic DNA

A 465-bp mouse *Fgf2* cDNA probe (kindly provided by J. Hébert [40]) was P<sup>32</sup>-labeled and hybridized to a mouse genomic lambda library (derived from mouse strain 129SVJ). Double-positive phages were identified, isolated, replated and rescreened. DNA from phages was isolated, digested with *Not1*, and Southern blots were hybridized to P<sup>32</sup>-labeled probes specific for exon 1, exon 2 or exon 3. Following further restriction enzyme digestions, fragments were subcloned into pBluescript KS (Stratagene Europe, Amsterdam, The Netherlands) and analyzed. Sequence analyses was performed using *Fgf2*-specific or pBluescript-specific primers. Sequence information was deposited in GenBank (AY324448, AY324449, AY324450, AY324451).

### Constructs

**GFP constructs.** A DNA fragment coding for the 18-kDa FGF2 [41] and a DNA fragment coding for the three FGF2 isoforms were inserted in frame into the vectors pEGFP-N or pEGFP-C (Clontech, Basel, Switzerland). The cDNA fragment encoding the small FGF2 isoform was extracted from the vector pmbFGF [41] with *SacI/AluI* and inserted into *SacI/SmaI* sites of pEGFP-N3 to generate pATGGFP, or with *NcoI* (blunted with Klenow)/*PstI* and inserted into *XhoI* (blunted)/*SmaI* sites of pEGFP-C3 to generate pGFPATG. Vector pATGKpGFP was constructed by isolating the insert with *SacI/KpnI* from pmbFGF and subcloning it into pEGFP-N2 digested with *SacI/KpnI*. Vectors pGFPATGKp or pGFPATGB were obtained by digesting pGFPATG with *KpnI* and *BamHI*, respectively, blunting the ends and religating the fragments. A *KpnI/EcoRV* fragment isolated from pmbFGF was inserted into pEGFP-C2 digested with *KpnI/SmaI* to generate pGFPKpTGA. Vector pGFPKpB was obtained by *BamHI* digestion of pGFPKpTGA followed by religation. The vectors pGFPATG1 and pGFPATG21 were generated from pGFPATG by PCR amplification with mismatched oligonucleotides. In both vectors, the 5' primer allowed amplification of part of the pEGFP-C3 polylinker including the *BglIII* site. In pGFPATG1, the 3' primer introduced a *BamHI* site and in pGFPATG21 an *ApaI* site. This enabled the PCR product to be introduced in pEGFP-C3 via these sites. Vectors pGFPATG3 and pGFPATG4 were generated by introduction of a stop codon by PCR amplification, followed by

ligation (*Bgl*III/*Eco*RI) into pEGFP-C3. The N-terminal extension containing the two alternative translation start sites which encode for the two HMW forms was extracted from a genomic DNA fragment (construct p65RR4ex1) derived from phage 65, containing exon 1 with 5' and 3' flanking regions. A DNA fragment containing the first 40 bp of exon 1 and 300 bp of its 5' region was extracted from p65RR4ex1 with *Nar*I and subcloned into pmbFGF2 digested with *Cl*aI/*Nar*I to generate vector pCTGbFGF. The fragment encoding the three isoforms was then isolated from pCTGbFGF with *Eco*RI/*Xho*I and inserted into pEGFP-N1 or pEGFP-C3 digested with *Eco*RI/*Xho*I to generate pCTGGFP or pGFPCTG. Vectors pGFPCTGB, pGFPCTGKp and pGFPCTGSma were generated by digesting pGFPCTG with *Bam*HI, *Kpn*I or *Sma*I, respectively, and religating the vectors. pGFPCTGNa was constructed by isolating the fragment from pGFPCTG with *Xho*I/*Nar*I and inserting it into pEGFP-C3 digested with *Xho*I/*Acc*I. To generate pCTGKpGFP, the fragment was isolated from pCTGGFP with *Kpn*I and inserted into pEGFP-N1 digested with *Kpn*I. The cDNA fragment encoding the four human FGF2 isoforms (vector pA [42]) was provided by Sophie Javerzat (Bordeaux, France). An *Nco*I (blunt)/*Eco*RI fragment from this pA vector was inserted into pEGFP-C1 digested with *Bgl*III (blunt)/*Eco*RI to generate pGFPPhATG. The *Xho*I/*Eco*RI fragment from pA was inserted into pEGFP-C2 digested with *Xho*I/*Eco*RI to generate pGFPPhCTG. More specific details on the cloning are available on request. Cloning and PCR amplification of all constructs was corroborated by sequence analysis to ascertain correct in-frame fusion and absence of undesired mutations.

**Flag constructs.** For the generation of pATGflag, cDNA encoding the 18-kDa isoform was retrieved from pmbFGF with *Xho*I/*Eco*RI, made blunt and inserted into blunted *Hind*III/*Sma*I sites of the vector pJI090 (provided by Pascal Schneider, Institute of Biochemistry, University of Lausanne, Switzerland). pCTGflag was created by inserting the fragment *Xho*I/*Eco*RI (blunted) from pCTGbFGF into the pJI090 vector digested with *Hind*III (blunted)/*Sma*I.

**CMVFGF2 constructs.** pEGFP-N1 was digested with *Bam*HI/*Not*I, made blunt and religated to remove the GFP coding region (vector pCMVN1). A *Sac*I/*Eco*RI fragment from pmbFGF was inserted into pCMVN1 digested with *Sac*I/*Eco*RI to generate pCMVATG. A *Bgl*III/*Bam*HI fragment from pCTGGFP was inserted into pCMVN1 digested with *Bgl*III/*Bam*HI to generate pCMVATG.

### Transfection and immunofluorescence

NIH3T3 and 293T cells were grown in DMEM medium (Gibco-BRL, Basel, Switzerland) supplemented with 8% fetal calf serum (FCS), 100 U/ml penicillin and streptomycin, 1 mM Hepes (Gibco), and 1 mM mercaptoethanol (Sigma, St. Louis, Mo.) in a humidified 5% CO<sub>2</sub>/95% air

atmosphere. B16F10 cells were grown in MEM medium (Gibco-BRL) supplemented with 10% FCS, 100 U/ml penicillin and streptomycin and 0.1% glutamine. 293T and NIH3T3 cells were transfected using calcium phosphate precipitation. All antibody stainings were performed at room temperature (RT) in six-well plates. Cells were grown on coverslips coated with poly-D-lysine (0.1 mg/ml) (Sigma) and fixed for 20 min in 4% paraformaldehyde. After quenching with 50 mM NH<sub>4</sub>Cl<sub>2</sub> in phosphate-buffered saline (PBS) for 5 min, the cells were permeabilized with 0.1% Tween 20 (Fluka, Buchs, Switzerland) for 5 min. Thereafter, the cells were incubated at 37°C with RNase (200 mg/ml) for 30 min, DNA was stained with propidium iodide (0.7 µg/ml) for 1 min and cells were mounted with 2.5% 1,4-diazabicyclo(2,2,2)octane (DABCO) (Fluka), (w/v) in 10% PBS, and 90% glycerol (98% solution). After permeabilization with Tween 20, nonspecific binding sites were blocked for 30 min with 10% goat serum in PBS. The cells were then incubated for 30 min with the primary antibody, for 30 min with the secondary antibody, and mounted in DABCO. Between each step, the cells were washed twice with PBS. Confocal microscopy of cells was performed on a Zeiss (Göttingen, Germany) Axiovert 100 microscope (Zeiss Laser Scanning Microscope 410) with a ×63 Plan-Apochromat objective (1.4 oil). To detect propidium iodide, a helium laser was filtered at 543 nm. An argon laser was used to detect GFP or fluorescein fluorochrome. Images were processed with Photoshop version 5.0 software (Adobe Systems Inc., San José, Calif.).

### Western blots

Transfected 293T cells were washed twice with ice-cold PBS, placed on ice and scraped in cold extraction buffer (20 mM Tris-HCl pH 7.5, 1% NP-40, 0.5% deoxycholate, 0.5 mM EDTA). Cell suspensions were transferred into Eppendorf tubes. Cells were additionally lysed by a cycle of freezing at -20°C and thawing at RT, followed by sonication. Protein content was evaluated by the Bradford assay (Bio-Rad, Reinach, Switzerland). Western blot analysis was performed according to standard procedures. Total protein extracts were boiled for 5 min in reducing SDS-PAGE sample buffer and electrophoresed on 15% SDS-polyacrylamide gels. The proteins were transferred to a nitrocellulose membrane which was blocked for nonspecific binding in PBS containing 4% lactate and 0.5% Tween 20 at RT for 1 h. Membranes were incubated with the primary antibody against FGF2 for 45 min, washed (4 × 1 min) with PBS-4% lactate-0.5% Tween 20, and incubated with the secondary antibody for 30 min. Finally, the membrane was washed (4 × 15 min) with PBS-0.5% Tween 20 and bands were visualized by a chemiluminescent reaction (ECL; Amersham Life Science, Otelfingen, Switzerland).

Mouse anti-Flag antibody M2 (kindly provided by Pascal Schneider, Institute of Biochemistry, University of Lausanne, Switzerland) was used at a dilution of 1/200. The rabbit anti-bovine FGF2 antibody was obtained from Sigma and used at 1/2000 dilution for immunoblotting detection or at 1/200 dilution for immunofluorescence. The secondary antibodies, goat anti-mouse conjugated to fluorescein (DTAF; diluted 1/400), donkey anti-rabbit conjugated to peroxidase (diluted 1/2000) or CY3 conjugated to affinitipure goat anti-rabbit IgG (diluted 1/400), were obtained from Jackson ImmunoResearch Laboratories Inc., West Grove, Pa.

### Heparin-sepharose purification of FGF2-GFP fusion protein

Transiently transfected 293T cells grown to subconfluence were washed with PBS, scraped, centrifuged and resuspended in cold extraction buffer (20 mM Tris-HCl pH 7.5, 1% NP-40, 0.5% deoxycholate, 0.5 mM EDTA). Cells were additionally lysed by a cycle of freezing at  $-20^{\circ}\text{C}$  and thawing at room temperature, followed by sonication. The cell debris was pelleted by centrifugation at 15,000 rpm for 15 min. The supernatant was applied to a heparin-sepharose beads column (Pharmacia, Uppsala, Sweden) in a 1-ml syringe. The column was washed with cold extraction buffer and the heparin-binding proteins were eluted with extraction buffer containing an increasing concentration of NaCl (0.5, 1, 1.5, 2 and 3 M). GFP fluorescence of eluted fractions was measured in 96-well plates with a microplate fluorometer (Packard Instrument Co., Meriden, Conn.).

## Results

### Mouse *Fgf2* genomic structure and N-terminal extension

The *Fgf2* gene locus was isolated and characterized using phages. These were subcloned and characterized by restriction map and partial sequencing, and were compared to the available sequence of the *Fgf2* cDNA coding for LMW FGF2. Sequencing of the intron-exon boundaries and high homology to the consensus splicing-site sequences confirmed the predicted exon size and exon-intron boundaries (not shown). The genomic organization of the mouse *Fgf2* gene is similar to that of the human *FGF2* gene. The three small exons (exon 1 175 bp, exon 2 104 bp, exon 3 186 bp) are separated by two large introns. Because of the absence of overlapping phages the precise size of intron 1 was not established but is estimated to be at least 18 kb; intron 2 is 8 kb long. To analyze the possible N-terminal extension, the upstream sequence of the common translational start site (ATG) was subcloned and analyzed. Alignment of 700 bp with the corresponding region of rat *Fgf2* [43] showed extensive

homology (not shown). Two potential alternative translation start sites correspond to the putative CTG start site of the rat (fig. 1a). Analysis of the *Fgf2* promoter sequence confirmed the absence of TATA or CAAT box sequence and a high content of GC.

### FGF2 HMW as well as LMW forms drive GFP to the nucleus

To analyze the distribution of FGF2 isoforms and identify domains involved in intracellular localization, we performed transfection studies with a series of GFP-tagged FGF2 fragments. For control experiments, GFP-coding sequence was either eliminated or substituted with a flag tag group. For expression of the 18-kDa isoform we used the corresponding mouse cDNA. Correct expression of the three isoforms and fusion proteins was confirmed by Western blot (fig. 1b).

To analyze the subcellular localization of the different fusion proteins, constructs were expressed in human embryonic kidney 293T cells and mouse NIH3T3 fibroblasts and examined by confocal microscopy (fig. 2). We obtained the same results for both cell lines. The first transfection experiments already revealed that GFP localization was influenced by the fusion with FGF2. While the GFP protein showed the expected unspecific localization when expressed alone, expression of all the isoforms was able to induce a nuclear localization of GFP. Fusion with the small isoform (ATGGFP) localized GFP to the nucleus, and a minor proportion to the cytoplasm. The 22-kDa isoform fused to GFP (GFPCTG) showed a strong and exclusive nuclear/nucleolar localization.

When the three isoforms were coexpressed (CTGGFP), the resulting localization was a merged pattern of the two preceding constructs: light cytoplasmic and strong nuclear/nucleolar signals (fig. 2). The observed results were specific to FGF2 and not due to aberrant effects induced by the fusion with GFP protein. Immunostaining of FGF2 isoform expressed alone (CMVATG, CMVCTG) or fused to a flag tag group (ATGflag, CTGflag) showed the same cellular distribution. Localization was identical for the N- or C-terminal position of GFP (GFPATG vs ATGGFP). This localization was not mouse specific and was identical to GFP fused to human FGF2 (GFPhATG, GFPhCTG). Again, the HMW forms localized specifically to the nucleus and the LMW form was found in the nucleus with some staining in the cytoplasm.

### Signals in the amino terminus of HMW forms of FGF2 lead to nuclear localization of a heterologous protein

To determine whether the N-terminal sequence of the mouse FGF2 mediates nuclear import, we generated a series of C-terminal deletion mutants (fig. 3). A first fusion construct of a deletion was made with GFP in the C-terminal position (CTGKpGFP), and resulted in nuclear and

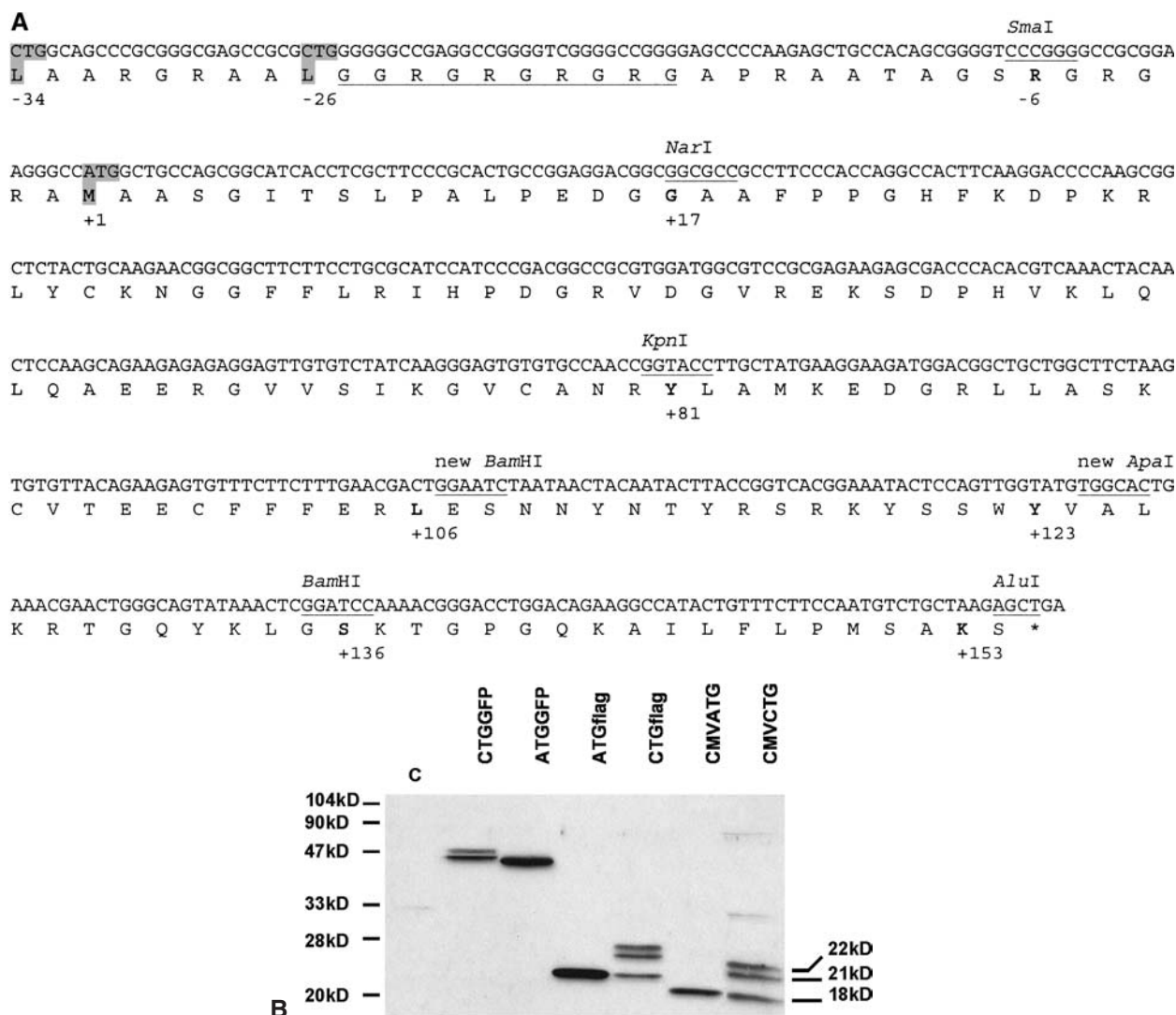


Figure 1. Mouse FGF2 contains two CTG translation initiation codons. (A) DNA sequence and deduced protein sequence of mouse FGF2, illustrating the two CTGs and the ATG (+1) (grey background). Existing restriction enzyme sites and new sites used for generation of constructs are indicated. Underlined sequence points to the proposed NLS for the HMW forms [44]. (B) Western blot analysis demonstrates the expression of the three isoforms (CMVATG, CMVCTG; 18 kDa, 21 kDa, 22 kDa). FGF2-flag (ATGflag, CTGflag) migrated at a slightly higher molecular weight, whereas FGF2-GFP (ATGGFP, CTGGFP) migrated at ~42 kDa and 45 kDa, 46 kDa (one band). See figure 2 for scheme of the constructs. C; control, untransfected 293T cells.

cytoplasmic staining (not shown). However, such constructs do not allow one to discriminate between CTG- and ATG-initiated forms. Thus, FGF2 fragments were fused in frame to GFP in the N-terminal position. Using confocal microscopy, we observed a gradual increase in the fluorescence in the cytoplasm when deleting the C terminus. All proteins with C termini ranging from 155 to 81 (GFPCTG, fig. 2; GFPCTGB, GFPCTGKp, fig. 3) localized exclusively to the nucleus. GFPCTGNa was found mostly in the nucleus but showed a very faint fluorescence in the cytoplasm, indicating that nuclear accumulation was less efficient. Within the nucleus, fluorescence seemed to colocalize with DNA (fig. 3). In contrast, GFPCTGSma localized homogeneously into all cell

compartments, indicating that further deletion of 23 amino acids from GFPCTGNa eliminated a specific sequence. This gradual loss in signal specificity may signify a loss of nuclear import/retention sequence or change of protein conformation.

#### Signals in the C-terminal region are essential for the nuclear localization of the 18-kDa isoform and for heparin binding

Despite the absence of the N-terminal NLS of the HMW form, constructs ATGGFP and GFPATG still resulted in nuclear localization (fig. 2), suggesting that other sequences in the FGF2 LMW form could be implicated in nuclear import and/or retention. To determine the possi-

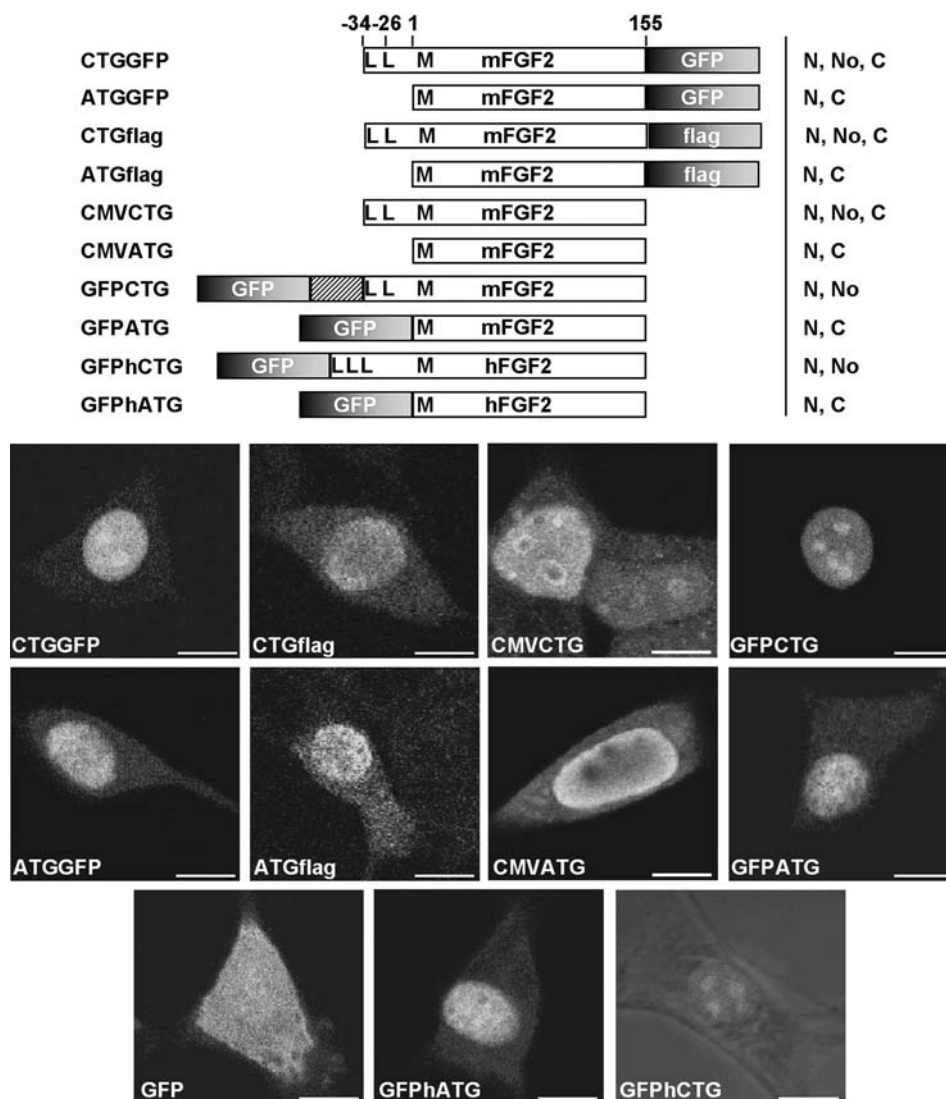


Figure 2. Intracellular localization of expressed FGF2 fusion proteins. Both LMW and HMW isoforms (CMVCTG, CMVATG) show nuclear localization and this is reproduced in fusions to flag, and in N-terminal and C-terminal fusions to GFP. The LMW form shows an additional weak fluorescence in the cytoplasm. Constructs are depicted with start sites indicated in bold (L, leucine; M, methionine); methionine (AUG translation start site) is referred as +1. Overall patterns are summarized alongside each construct. N, nuclear, No, nucleolar, C, cytoplasmic. Bar, 10 μm.

ble importance of the carboxy terminus, we progressively deleted the C-terminal region of the GFPATG fusion protein (fig. 4). Examination of the subcellular localization showed two different patterns. In the shorter deletions, GFPATG4 and GFPATG3, with either 4 or 8 C-terminal amino acids missing, nuclear staining was abrogated and fluorescence was mostly perinuclear (fig. 4). Deletion of the last 19 or 32 amino acids (GFPATGB, GFPATG21; fig. 4) resulted in a similar localization pattern, but with a higher variability. In most of the cells (8 out of 10, construct GFPATGB), staining was perinuclear (fig. 4), but a few cells (2 out of 10) showed obviously unspecific staining (nuclear and cytoplasmic, not shown). This variability, which was not seen in other constructs (beside GF-

PATGB and GFPATG21), might be due to the generation of an unstable protein conformation or a partial accessibility/inaccessibility of an interacting factor. One common feature was the formation of very intense fluorescent spots which localized in the cytoplasm and on the boundary with the nucleus. When NIH3T3 cells were allowed to grow for 48 h after transfection, the spots grew in size and seemed to be harmful for the cells. The same phenomenon was observed in 293T cells but occurred much faster, due to higher transfection efficiency and/or more copies entering the cell. Further deletion of another 17 amino acids from the C terminus (GFPATG1) resulted in an unspecific localization and disappearance of the fluorescent spots (fig.4). This might suggest important sequences

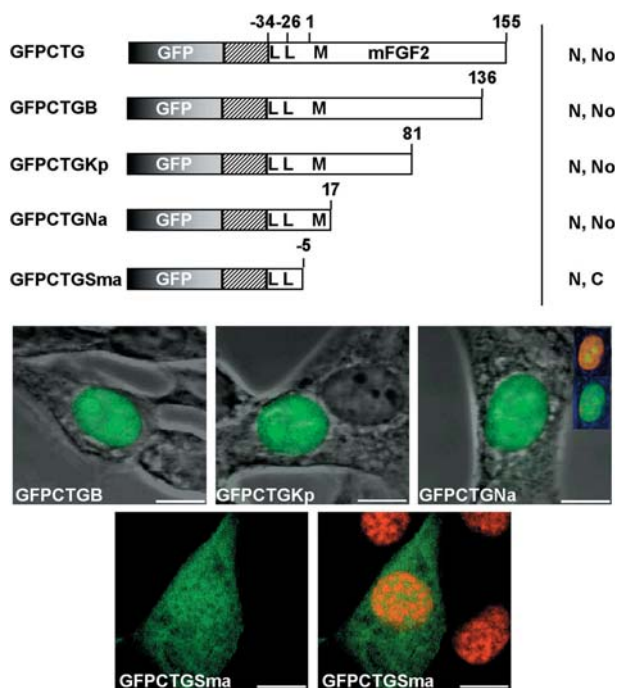


Figure 3. Influence of N-terminal sequences on subcellular localization of HMW FGF2. The N terminus of the mouse FGF2 HMW isoform is able to mediate nuclear localization in the absence of the C terminus. The different plasmids were introduced in NIH3T3 cells and subcellular distribution was analyzed by confocal microscopy. In GFPCTGSma, DNA was counterstained with propidium iodide (red staining). In GFPCTGNa, the insets depict GFP fluorescence (below) in comparison to a merge with propidium iodide counterstaining (above). Bar, 10  $\mu$ m. N, nuclear, No, nucleolar, C, cytoplasmic.

within this stretch of 17 amino acids. On the other hand, removal of these amino acids might render the protein rather unstable, since several  $\beta$ -strands are missing according to the three-dimensional structure of the protein [1, 45]. Remarkably, lack of a further 25 amino acids (GFPATGKp, ATGKpGFP) led to a consistent exclusion of nucleolar fluorescence (fig. 4). This effect was only seen with these 81 amino acids of FGF2, and thus whether a nucleolar localization or retention signal is missing, or whether a peculiar protein conformation is causing this effect is not clear.

One of the characteristics of FGFs is their heparin-binding capacity. We thus addressed this property and tested effects of different FGF2-GFP fusion constructs (fig. 5). Cell extracts of transiently transfected 293T cells were passed through heparin mini-columns and eluted with increasing NaCl molarity. Fluorescence of the eluted fractions was measured to monitor binding capacity of the fusion proteins. Fractionation showed that the heparin-binding affinity of the 18-kDa isoform was not altered by the presence of GFP and that the fusion proteins eluted at the expected NaCl molarity (1.5 M) (GFPATG; fig. 5). In contrast, deletion of the C-terminal four amino acids im-

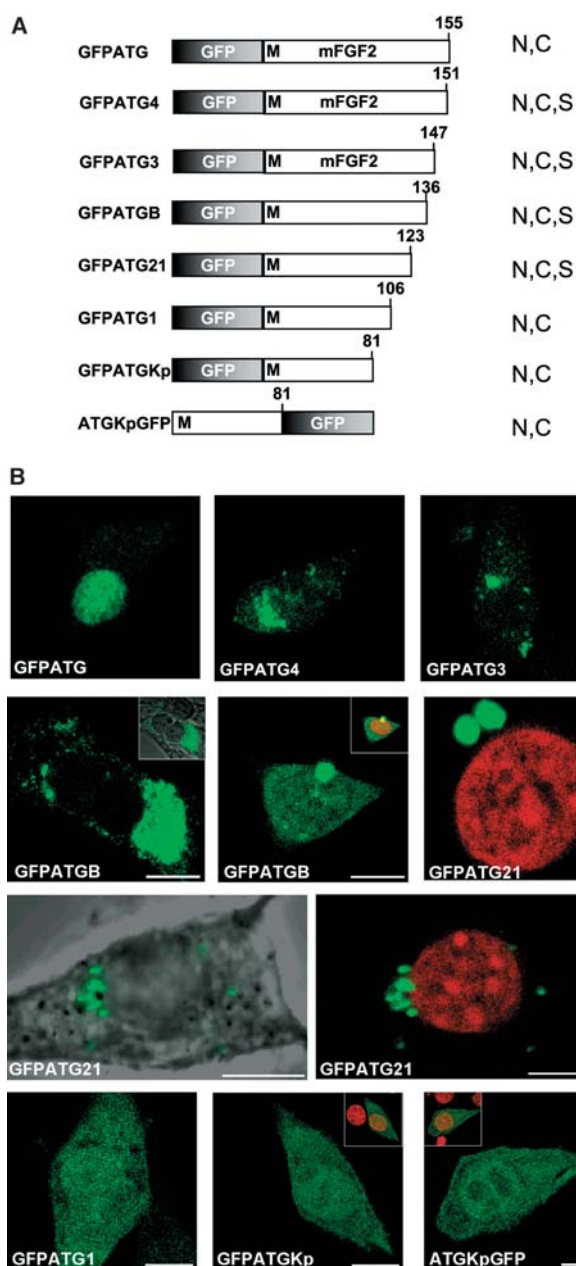


Figure 4. Influence of C-terminal sequences on subcellular localization of the 18-kDa FGF2 isoform. Constructs carrying C-terminal deletions (GFPATG3, GFPATG4, GFPATGB, GFPATG21) reveal loss of specific nuclear localization and appearance of perinuclear/cytoplasmic fluorescent spots. Further deletions resulted in unspecific localization of fluorescence. Representative examples of localization are shown. Small insets depict red counterstaining of DNA with propidium iodide. The image of GFPATG (fig. 2) is depicted for comparison. Bar, 10  $\mu$ m. N, nuclear, No, nucleolar, C, cytoplasmic, S, juxtannuclear and reticular staining.

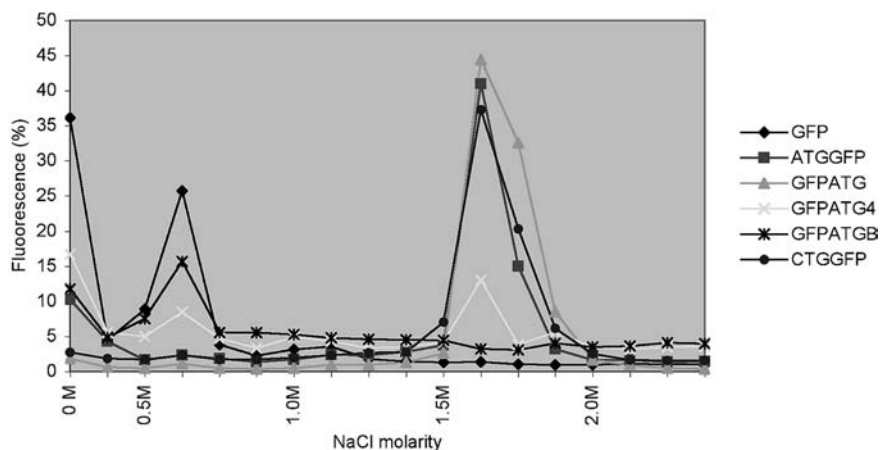


Figure 5. The FGF2 C-terminus is required for heparin binding. Heparin-bound cell extracts of ATGGFP-, GFPATG- and CTGGFP-transfected cells eluted at 1.5 M NaCl, whereas C-terminal deletions severely affected this heparin-binding capacity. Constructs are depicted in figures 2 and 4.

paired the heparin-binding capacity of FGF2 (GFPATG4), and following further deletion (GFPATGB), heparin binding was barely detectable.

Since the last 74 amino acids of FGF2 seemed to contain domains relevant for nuclear localization, we tested whether this sequence is sufficient to direct localization of a heterologous protein. C-terminal fragments were subcloned to GFP (fig. 6). GFPKpTGA and GFPKpB distributed broadly into the cell and formed small fluorescent spots, similarly to GFPATGB (fig. 4), but of smaller size. In addition, GFPKpTGA was not able to retain any heparin binding (not shown). Further removal of 13 amino acids (GFPKp2) from the C terminus of GFPKpB or subcloning of the last 18 amino acids (GFPBTGA) resulted in localization indistinguishable from GFP alone (fig. 2), suggesting that the C terminus alone is not sufficient for nuclear localization.

## Discussion

The biological function of at least 15 members of the FGF family has now been addressed by homologous recombination in the mouse, with phenotypes ranging from early embryonic lethality to subtle phenotypes [1]. Such gene-targeting experiments not only allow one to address roles of these growth factors in physiology and development, but also in cancer research and with respect to human disease models. Moreover, they might enable the introduction of specific mutations allowing modification of the intracellular localization of the proteins. In such an experiment, we recently replaced the C-terminal part of FGF2 by an in-frame fusion to a lacZ coding sequence (*Fgf2<sup>tm1Bee</sup>* [38]), identical to CTGKpGFP or ATGKpGFP (fig. 4). Deletion of the C-terminal half of FGF2 in vivo was sufficient to abolish FGF2 function [38, 39]. Expres-

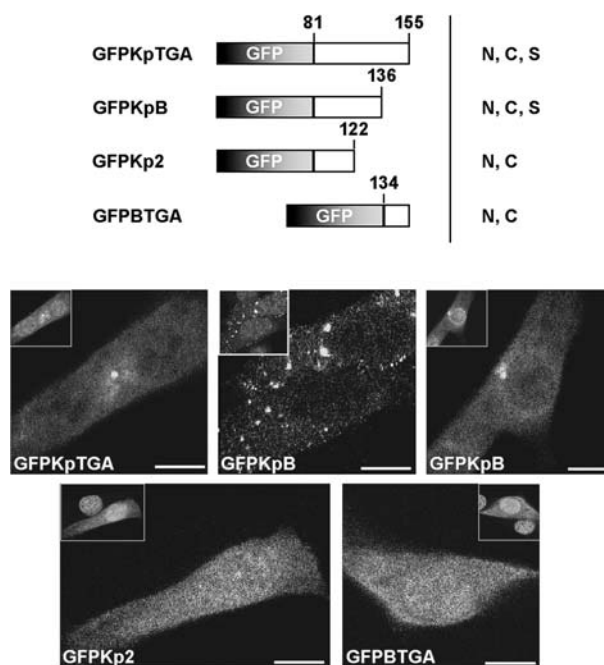


Figure 6. Intracellular localization by C-terminal sequences alone. Fusions of GFP to fragments of the C terminus or to the C-terminal half of FGF2 do not result in nuclear localization. The different plasmids were transfected into NIH3T3 cells and subcellular distribution of fusion proteins was analyzed by confocal microscopy. Representative examples of localization are shown. Small insets depict red counterstaining of DNA with propidium iodide. Bar, 10  $\mu$ m. N, nuclear, C, cytoplasmic, S, juxtannuclear and reticular staining.

sion from this FGF2-lacZ fusion gene was only seen in cartilage, and at a cellular level, the lacZ staining was found in both the nucleus and cytoplasm of the positive cells. These data illustrated that a fusion gene with FGF2 in the N-terminal position is expressed in mice, but is biologically not functional in the absence of the last 74 amino acids.



We now linked these transgenic experiments to experiments in cell culture and addressed the intracellular localization of FGF2 in fusion to GFP. Initial experiments were concordant with published results from human FGF2 (and of other vertebrates) and demonstrate that the HMW forms of mouse FGF2 are able to drive GFP to the nucleus. However, these experiments also showed that this characteristic was not restricted to the HMW forms, since LMW-GFP fusion protein equally localized to the nucleus with only a minor proportion in the cytoplasm. This localization was also found for GFP fusion proteins, using the human FGF2 protein. To confirm these results, cells were transfected with vectors expressing FGF2 proteins alone or fused to a flag tag group. Immunofluorescence detection confirmed the localization of GFP fusion proteins suggesting that GFP did not cause aberrant effects. This is also supported by recent data, where both N- and C-terminal fusion of GFP to rat FGF2 (the 18-kDa form) did not affect correct export of the protein [41]. We thus suggest that the small isoform of FGF2 (LMW, 18 kDa) is essentially located in the nucleus.

To elucidate the localization of FGF2 in more detail, we generated a series of C-terminal deletions of the HMW form. We showed that amino acids between position -6 and +17 (GFPCTGSma, GFPCTGNa) play an essential role in the nuclear localization of the HMW isoforms. The entire N-terminal extension of the HMW has been shown to target  $\beta$ -galactosidase to the nucleus but not to the nucleolus [8]. Sequence comparison of the FGF2 protein sequence from different vertebrate species showed that several glycine-arginine repeats of varying length are present in the amino-terminal part. One of these motifs (fig. 1) was shown to increase the nuclear accumulation about threefold if inserted in the amino-terminal part of the small isoform [44]. The N-terminal sequence is now well recognized as a NLS, and recent data have shown that posttranslational modifications which include methylation of the arginines are essential for nuclear localization. In the absence of methylation, HMW FGF2 is equally distributed between cytoplasm and nucleus [11]. A first step into the understanding of differential functions (or localization) might be the identification of proteins specifically binding to the HMW isoform, as for example the exclusive coimmunoprecipitation and colocalization with survival of motoneuron protein (SMP) in rat Schwann cells [46]. The HMW form, but not the LMW form has also been reported to specifically associate with chromatin and histone H1 [47].

The nuclear accumulation of the small isoform suggests a synergistic interaction of several signals. Apparently, two separate signals, the amino-terminal extension and a putative nucleolar localization sequence within the LMW sequence, are needed for nuclear and nucleolar localization of the HMW FGF2 forms. Nucleolar localization of FGF2 has been reported both for the long and the short

isoforms, and the nucleolar localization sequence was postulated as being distinct from NLSs [33]. On the other hand, elegant experiments on FGF3 have demonstrated a nucleolar binding of FGF3 to the protein NoBP, mediated by the C terminus and the same sequences as required for the nuclear localization [48]. From our experiments, a nucleolar signal is conceivably located in region +1 to +17. Nevertheless, this nucleolar signal does not seem to be sufficient to mediate nucleolar localization in the absence of a nuclear localization sequence (GFPATGKp, ATGKpGFP; fig. 4). Feasibly, the nucleolar localization of the LMW isoform is equally linked to its NLS, as reported for FGF3 [48].

By progressive deletion of the LMW form, we could show that the C-terminal region is essential for correct nuclear localization and heparin binding. Deletion of the last 4 (GFPATG4), 8 (GFPATG3), 19 (GFPATGB) or 32 amino acids (GFPATG21) abrogated the specific nuclear localization and induced juxtannuclear or reticular localization of GFP fusion proteins. Removal of a further 17 (GFPATG1) or 42 amino acids (GFPATGKp) resulted in a very homogenous and unspecific distribution. Nevertheless, the C terminus was not sufficient for nuclear localization and heparin binding (GFPKpTGA). From this experiment, we suggest that the C terminus contains an essential element that is not functional without the interaction with other parts of the protein. In concordance with our data, point mutations of arginines at position +115 and +117 (R149G, R151G) within a conserved C-terminal sequence of FGF2 (R149G, R151G; fig. 7) led to cytoplasmic localization in fusions to red fluorescent protein in Schwann cells [46]. Equally, deletion of the last 6 or 9 amino acids at the C terminus of FGF1 impaired receptor and heparin binding [49].

The findings raise the question of the mechanism(s) responsible for nuclear accumulation of the 18-kDa isoform observed both in transient and in stable transfectants. The subcellular fate of FGF3 is controlled by competition of a bipartite NLS with a secretory signal located near the amino terminus [48, 50]. A functional NLS in the carboxyl terminus was confirmed by fusing it to  $\beta$ -galactosidase and targeting the chimeric protein to the nucleus [51]. FGF1 also accumulates in the nuclei, and deletion of an NLS abolishes nuclear translocation [52, 53]. Localization of FGF2 may be regulated following a similar mechanism, even though classical NLSs seem to be missing. Nevertheless, the few amino acid motifs (for example YNTY; fig. 7) which are homologous between different FGFs might be implicated. This is supported by the effect of point mutations in the neighboring amino acids (see above [46]). Insertion of point mutations in residues +27 to +31 of the human FGF2, which is in good agreement with a consensus sequence for nuclear translocation [54], did not impair the nuclear localization of the 18-kDa isoform [55]. Mutants retained their receptor binding and mitogenic capacity but

		82	106	123
mouse	FGF2	LAMKEDGRLLASKCVTEECFFFERLESNNYNTYRSRKY . . . . . S . . SWYVALKRT		
human	FGF2	LAMKEDGRLLASKCVTDECFERLESNNYNTYRSRKY . . . . . T . . SWYVALKRT		
mouse	FGF1	LAMDEGLLYGSQTPNEECLFLERLEENHYNTYTSKKH . . . . . AEKNWFVGLKKN		
human	FGF3	LAMNKRGRLYASEHYSAECEFVERIHELGYNTYASRLYRTVSSTPGARRQPSAERLWYVSVNGK		
mouse	FGF3	LAMNKRGRLYASDHNAECEFVERIHELGYNTYASRLYRTGSSGPGAQRQPGAQRPWVSVNGK		
mouse	FGF9	LGMNEKGELYGSEKLTQECVFREQFEENWYNTYSSNLYKHVDT . . G . . R . . . . . R . YYVALNKD		
Consensus		L-M- - -G-L- - -S- - - - -EC-F-E- - - - -YNTY-S- - - - - - - - - - - - - - - - -V- - - - -		
		136	154	
mouse	FGF2	GQYKLGSKTGPQKAILFLPMSAKS *		
human	FGF2	GQYKLGSKTGPQKAILFLPMSAKS *		
mouse	FGF1	GSCKRGPRTHYGQKAILFLPLPVSSD *		
human	FGF3	GRPRRGFKTRRTQKSSLFLPRVLD . HRDHEMVR . QL . QSGLP RP PGKGVQPRRRRQ . KQS		
mouse	FGF3	GRPRRGFKTRRTQKSSLFLPRV LG . HKDHEMVR . LL . QSSQPRAPEGGSQPRQRQKQKQS		
mouse	FGF9	GTPREGTRTKRHQKFTHFLPRVDPDKVPELYKDILSQS *		
Consensus		G- - - -G- - -T- - - -QK- - - -FLP- -		

Figure 7. Protein sequence of the C terminus of the FGF family. Alignment of the C-terminal amino acids of mouse and human FGF2, FGF1, FGF3 and FGF9 (mouse only) reveals only very few highly conserved amino acids. Note that constructs pGFPATG4 and pGFPATG3 lack only the last 4 or 8 amino acids, respectively, including the conserved FLP sequence (pGFPATG3). Numbering refers to the protein sequence of mouse FGF2 (ATG = +1). Asterisk indicates stop codon: The C-terminal sequence of FGF3 is not indicated completely.

had a 100-fold reduced urokinase-type plasminogen activator capacity. Interestingly, this latter activity was restored by addition of soluble heparin [55]. Similar results on the biological activity of FGF2 were obtained with another mutant in which residues in different regions of FGF2 were mutated, suggesting that alteration of the tertiary structure rather than of the primary structure of the protein is responsible for these modifications [56].

Neither N-terminal region (ATGKpGFP; fig. 4), C-terminal region (GFPKpTGA; fig. 6) nor fusions of the entire 18-kDa isoform with the other reporter genes (chloramphenicol acetyltransferase [6]; pyruvate kinase [44]) were able to locate to the nucleus, thus indicating that the LMW isoform does not contain a simple NLS and correct localization thus depends on a tight interaction between N and C termini. Nuclear localization of the 18-kDa isoform might thus be dependent on the intact three-dimensional structure and less or not at all on the presence of a specific NLS. Many small proteins enter the nucleus by diffusion rather than by NLS and energy-dependent mechanisms. The 18-kDa isoform might thus diffuse into the nucleus through the nuclear pore and bind to chromatin, staying in the nuclear compartment during the interphase [55]. The protein structure of FGF2 has been known for nearly a decade and is composed of a  $\beta$  trefoil structure with four-stranded  $\beta$ -sheets in a triangular array [1, 45, 57]. The N-terminal and the C-terminal part of the protein are juxtaposed and are both part of the same  $\beta$ -sheet. Thus, certain modifications in the C terminus might directly affect the structure of this  $\beta$ -sheet. In contrast, the N-terminal extension of the HMW forms seems not to participate in the structure, and is probably accessible as an NLS independent of most changes in the protein core. Heparin-binding regions are located around  $\beta$ -strands 10 and 11, and do not overlap with the sites binding to the receptor [1, 58].

The 18-kDa isoform might be first secreted to the cell surface before being transported to the nucleus. Localization might depend on association with other proteins, which is tightly dependent on the three-dimensional structure. FGFR and heparan sulfate proteins were shown to translocate to the nucleus and might be implicated in this alternative signaling pathway. They might be actively implicated in nuclear transport acting as carrier proteins [22, 49]; alternatively, their functions might be to stabilize and protect FGF2 proteins without affecting free diffusion [59]. Recently, a protein implicated in trafficking internalized FGF2, translokine, has been demonstrated to bind between  $\beta$  strands 2 and 5 and between  $\beta$  strands 8 and 10 [60]. The latter includes amino acids 103–126, which might explain the lack of any specific localization, when comparing GFPATG21 and GFPATG1 (fig. 4). If binding of FGF2 to HSPGs is required for nuclear localization, as demonstrated recently [49], any effect on one of the heparin-binding sites ( $\beta$  strands 1 and 2,  $\beta$  strands 10 and 11 [1]) will affect nuclear localization. Since even the smallest C-terminal deletions (GFPATG4) affected heparin binding (fig. 6), this might explain the loss of nuclear localization (fig. 4) as well.

In summary, we have characterized the mouse FGF2 and its intracellular localization. While the N terminus is essential for nuclear localization of the HMW isoforms, the C terminus is only important for nuclear localization of the LMW isoform, possibly by interacting with N-terminal sequences of the protein.

**Acknowledgements.** This work was supported by funds from the Swiss National Science Foundation, the Swiss Cancer League and NCCR Molecular Oncology. Thanks are due to S. Poncet for initial help in cloning mouse *Fgf2* 5' sequences, to C. Ruegg for support, to S. Javerzat and P. Schneider for reagents and to E. Hummler for comments on the manuscript.

- 1 Ornitz D. and Itoh N. (2001) Fibroblast growth factors. *Genome Biol.* **2**: 3005.3001–3005.3012
- 2 Arnaud E., Touriol C., Boutonnet C., Gensac M. C., Vagner S., Prats H. et al. (1999) A new 34-kilodalton isoform of human fibroblast growth factor 2 is cap dependently synthesized by using a non-AUG start codon and behaves as a survival factor. *Mol. Cell. Biol.* **19**: 505–514
- 3 Prats H., Kaghad M., Prats A. C., Klagsbrun M., Lelias J. M., Liauzun P. et al. (1989) High molecular mass forms of basic fibroblast growth factor are initiated by alternative CUG codons. *Proc. Natl. Acad. Sci. USA* **86**: 1836–1840
- 4 Florkiewicz R. Z. and Sommer A. (1989) Human basic fibroblast growth factor gene encodes four polypeptides: three initiate translation from non-AUG codons. *Proc. Natl. Acad. Sci. USA* **86**: 3978–3981
- 5 Renko M., Quarto N., Morimoto T. and Rifkin D. B. (1990) Nuclear and cytoplasmic localization of different basic fibroblast growth factor species. *J. Cell. Physiol.* **144**: 108–114
- 6 Bugler B., Amalric F. and Prats H. (1991) Alternative initiation of translation determines cytoplasmic or nuclear localization of basic fibroblast growth factor. *Mol. Cell. Biol.* **11**: 573–577
- 7 Florkiewicz R. Z., Baird A. and Gonzalez A. M. (1991) Multiple forms of bFGF: differential nuclear and cell surface localization. *Growth Factors* **4**: 265–275
- 8 Quarto N., Finger F. P. and Rifkin D. B. (1991) The NH<sub>2</sub>-terminal extension of high molecular weight bFGF is a nuclear targeting signal. *J. Cell. Physiol.* **147**: 311–318
- 9 Pintucci G., Quarto N. and Rifkin D. B. (1996) Methylation of high molecular weight fibroblast growth factor-2 determines post-translational increases in molecular weight and affects its intracellular distribution. *Mol. Cell. Biol.* **7**: 1249–1258
- 10 Burgess W. H., Bizik J., Mehlman T., Quarto N. and Rifkin D. B. (1991) Direct evidence for methylation of arginine residues in high molecular weight forms of basic fibroblast growth factor. *Cell Regul.* **2**: 87–93
- 11 Arese M., Chen Y., Florkiewicz R. Z., Gualandris A., Shen B. and Rifkin D. B. (1999) Nuclear activities of basic fibroblast growth factor: potentiation of low-serum growth mediated by natural or chimeric nuclear localization signals. *Mol. Biol. Cell* **10**: 1429–1444
- 12 Mignatti P., Morimoto T. and Rifkin D. B. (1992) Basic fibroblast growth factor, a protein devoid of secretory signal sequence, is released by cells via a pathway independent of the endoplasmic reticulum-Golgi complex. *J. Cell. Physiol.* **151**: 81–93
- 13 Florkiewicz R. Z., Majack R. A., Buechler R. D. and Florkiewicz E. (1995) Quantitative export of FGF-2 occurs through an alternative, energy-dependent, non-ER/Golgi pathway. *J. Cell. Physiol.* **162**: 388–399
- 14 Bikfalvi A., Klein S., Pintucci G., Quarto N., Mignatti P. and Rifkin D. B. (1995) Differential modulation of cell phenotype by different molecular weight forms of basic fibroblast growth factor: possible intracellular signaling by the high molecular weight forms. *J. Cell Biol.* **129**: 233–243
- 15 Bouche G., Gas N., Prats H., Baldin V., Tauber J. P., Teissie J. et al. (1987) Basic fibroblast growth factor enters the nucleolus and stimulates the transcription of ribosomal genes in ABAE cells undergoing G<sub>0</sub>–G<sub>1</sub> transition. *Proc. Natl. Acad. Sci. USA* **84**: 6770–6774
- 16 Baldin V., Roman A. M., Bosc B. I., Amalric F. and Bouche G. (1990) Translocation of bFGF to the nucleus is G<sub>1</sub> phase cell cycle specific in bovine aortic endothelial cells. *EMBO J* **9**: 1511–1517
- 17 Gualandris A., Urbinati C., Rusnati M., Ziche M. and Presta M. (1994) Interaction of high-molecular-weight basic fibroblast growth factor with endothelium: biological activity and intracellular fate of human recombinant M(r) 24,000 bFGF. *J. Cell. Physiol.* **161**: 149–159
- 18 Gualandris A., Coltrini D., Bergonzoni L., Isacchi A., Tenca S., Ginelli B. et al. (1993) The NH<sub>2</sub>-terminal extension of high molecular weight forms of basic fibroblast growth factor (bFGF) is not essential for the binding of bFGF to nuclear chromatin in transfected NIH 3T3 cells. *Growth Factors* **8**: 49–60
- 19 Tessler S. and Neufeld G. (1990) Basic fibroblast growth factor accumulates in the nuclei of various bFGF-producing cell types. *J. Cell. Physiol.* **145**: 310–317
- 20 Stachowiak M. K., Maher P. A., Joy A., Mordechai E. and Stachowiak E. K. (1996) Nuclear accumulation of fibroblast growth factor receptors is regulated by multiple signals in adrenal medullary cells. *Mol. Biol. Cell* **7**: 1299–1317
- 21 Stachowiak M. K., Maher P. A., Joy A., Mordechai E. and Stachowiak E. K. (1996) Nuclear localization of functional FGF receptor 1 in human astrocytes suggests a novel mechanism for growth factor action. *Brain Res. Brain Res. Prot.* **38**: 161–165
- 22 Stachowiak E. K., Maher P. A., Tucholski J., Mordechai E., Joy A., Moffett J. et al. (1997) Nuclear accumulation of fibroblast growth factor receptors in human glial cells – association with cell proliferation. *Oncogene* **14**: 2201–2211
- 23 Givol D. and Yayon A. (1992) Complexity of FGF receptors: genetic basis for structural diversity and functional specificity. *FASEB J.* **6**: 3362–3369
- 24 Giordano S., Sherman L., Lyman W. and Morrison R. (1992) Multiple molecular weight forms of basic fibroblast growth factor are developmentally regulated in the central nervous system. *Dev. Biol.* **152**: 293–303
- 25 Liu L., Doble B. W. and Karami E. (1993) Perinatal phenotype and hypothyroidism are associated with elevated levels of 21.5- to 22-kDa basic fibroblast growth factor in cardiac ventricles. *Dev. Biol.* **157**: 507–516
- 26 Dono R. and Zeller R. (1994) Cell-type-specific nuclear translocation of fibroblast growth factor-2 isoforms during chicken kidney and limb morphogenesis. *Dev. Biol.* **163**: 316–330
- 27 Vagner S., Touriol C., Galy B., Audigier S., Gensac M. C., Amalric F. et al. (1996) Translation of CUG- but not AUG-initiated forms of human fibroblast growth factor 2 is activated in transformed and stressed cells. *J. Cell Biol.* **135**: 1391–1402
- 28 Coffin J., Florkiewicz R., Neumann J., Mort-Hopkins T., Dorn II G., Lightfoot P. et al. (1995) Abnormal bone growth and selective translational regulation in basic fibroblast growth factor (FGF-2) transgenic mice. *Mol. Biol. Cell* **6**: 1861–1873
- 29 Kamiguchi H., Yoshida K., Wakamoto H., Inaba M., Sasaki H., Otani M. et al. (1996) Cytokine-induced selective increase of high-molecular-weight bFGF isoforms and their subcellular kinetics in cultured rat hippocampal astrocytes. *Neurochem. Res.* **21**: 701–706
- 30 Gualandris A., Arese M., Shen B. and Rifkin D. B. (1999) Modulation of cell growth and transformation by doxycycline-regulated FGF-2 expression in NIH-3T3 cells. *J. Cell Physiol.* **181**: 273–284
- 31 Nesbit M., Nesbit H. K., Bennett J., Andl T., Hsu M. Y., Dejesus E. et al. (1999) Basic fibroblast growth factor induces a transformed phenotype in normal human melanocytes. *Oncogene* **18**: 6469–6476
- 32 Vaccarino F., Schwartz M., Raballo R., Nilsen J., Rhee J., Zhou M. et al. (1999) Changes in cerebral cortex size are governed by fibroblast growth factor during embryogenesis. *Nat. Neurosci.* **2**: 246–253
- 33 Zhou M., Sutliff R., Paul R., Lorenz J., Hoying J., Haudenschild C. et al. (1998) Fibroblast growth factor 2 control of vascular tone. *Nat. Med.* **4**: 201–207
- 34 Dono R., Texido G., Dussel R., Ehmke H. and Zeller R. (1998) Impaired cerebral cortex development and blood pressure regulation in FGF-2-deficient mice. *EMBO J.* **17**: 4213–4225
- 35 Schultz J., Witt S., Nieman M., Reiser P., Engle S., Zhou M. et al. (1999) Fibroblast growth factor-2 mediates pressure-induced hypertrophic response. *J. Clin. Invest.* **104**: 709–719
- 36 Ortega S., Ittmann M., Tsang S., Ehrlich M. and Basilico C. (1998) Neuronal defects and delayed wound healing in mice

- lacking fibroblast growth factor 2. *Proc. Natl. Acad. Sci. USA* **95**: 5672–5677
- 37 Montero A., Okada Y., Tomita M., Ito M., Tsurukami H., Nakamura T. et al. (2000) Disruption of fibroblast growth factor-2 gene results in decreased bone mass and bone formation. *J. Clin. Invest.* **105**: 1085–1093
- 38 Foletti A., Ackermann J., Schmidt A., Hummler E. and Beermann F. (2002) Absence of fibroblast growth factor 2 does not prevent tumor formation originating from the RPE. *Oncogene* **21**: 1841–1847
- 39 Pellicieux C., Foletti A., Peduto G., Aubert J. F., Nussberger J., Beermann F. et al. (2001) Dilated cardiomyopathy and impaired cardiac hypertrophic response to angiotensin II in mice lacking FGF-2. *J. Clin. Invest.* **108**: 1843–1851
- 40 Hebert J. M., Basilico C., Goldfarb M., Haub O. and Martin G. R. (1990) Isolation of cDNAs encoding four mouse FGF family members and characterization of their expression patterns during embryogenesis. *Dev. Biol.* **138**: 454–463
- 41 Engling A., Backhaus R., Stegmayer C., Zehe C., Seelenmeyer C., Kehlenbach A. et al. (2002) Biosynthetic FGF-2 is targeted to non-lipid raft microdomains following translocation to the extracellular surface of CHO cells. *J. Cell Sci.* **115**: 3619–3631
- 42 Quarto N., Talarico D., Florkiewicz R. and Rifkin D. B. (1991) Selective expression of high molecular weight basic fibroblast growth factor confers a unique phenotype to NIH 3T3 cells. *Cell Regul.* **2**: 699–708
- 43 Pasumarthi K., Jin Y. and Cattini P. (1997) Cloning of the rat fibroblast growth factor-2 promoter region and its response to mitogenic stimuli in glioma C6 cells. *J. Neurochem.* **66**: 898–908
- 44 Dono R., James D. and Zeller R. (1998) A GR-motif functions in nuclear accumulation of the large FGF-2 isoforms and interferes with mitogenic signalling. *Oncogene* **16**: 2151–2158
- 45 Moy F. J., Seddon A. P., Bohlen P. and Powers R. (1996) High-resolution solution structure of basic fibroblast growth factor determined by multidimensional heteronuclear magnetic resonance spectroscopy. *Biochemistry* **35**: 13552–13561
- 46 Claus P., Döring F., Gringel S., Müller-Ostermeyer F., Fuhlrott J., Kraft T. et al. (2003) Differential intranuclear localization of fibroblast growth factor-2 isoforms and specific interaction with the survival of motoneuron protein. *J. Biol. Chem.* **278**: 479–486
- 47 Sun G., Doble B., Sun J., Fandrich R., Florkiewicz R., Kirshenbaum L. et al. (2001) CUG-initiated FGF-2 induces chromatin compaction in cultured cardiac myocytes and in vitro. *J. Cell. Physiol.* **186**: 457–467
- 48 Reimers K., Antoine M., Zapatka M., Blecken V., Dickson C. and Kiefer P. (2001) NoBP, a nuclear fibroblast growth factor 3 binding protein, is cell cycle regulated and promotes cell growth. *Mol. Cell. Biol.* **21**: 4996–5007
- 49 Miyakawa K., Ozawa K., Uruno T. and Imamura T. (1999) The C-terminal region of fibroblast growth factor-1 is crucial for its biological activity and high level protein expression in mammalian cells. *Growth Factors* **16**: 191–200
- 50 Kiefer P., Acland P., Pappin D., Peters G. and Dickson C. (1994) Competition between nuclear localization and secretory signals determines the subcellular fate of a single CUG-initiated form of FGF3. *EMBO J.* **13**: 4126–4136
- 51 Antoine M., Reimers K., Dickson C. and Kiefer P. (1997) Fibroblast growth factor 3, a protein with dual subcellular localization, is targeted to the nucleus and nucleolus by the concerted action of two nuclear localization signals and a nuclear retention signal. *J. Biol. Chem.* **272**: 29475–29481
- 52 Imamura T., Engleka K., Zhan X., Tokita Y., Forough R., Roeder D. et al. (1990) Recovery of mitogenic activity of a growth factor mutant with a nuclear translocation sequence. *Science* **249**: 1567–1570
- 53 Lin Y. Z., Yao S. Y. and Hawiger J. (1996) Role of the nuclear localization sequence in fibroblast growth factor-1-stimulated mitogenic pathways. *J. Biol. Chem.* **271**: 5305–5308
- 54 Chelsky D., Ralph R. and Jonak G. (1989) Sequence requirements for synthetic peptide-mediated translocation to the nucleus. *Mol. Cell. Biol.* **9**: 2487–2492
- 55 Presta M., Gualandris A., Urbinati C., Rusnati M., Coltrini D., Isacchi A. et al. (1993) Subcellular localization and biological activity of M(r) 18,000 basic fibroblast growth factor: site-directed mutagenesis of a putative nuclear translocation sequence. *Growth Factors* **9**: 269–278
- 56 Presta M., Statuto M., Isacchi A., Caccia P., Pozzi A., Gualandris A. et al. (1992) Structure-function relationship of basic fibroblast growth factor: site-directed mutagenesis of a putative heparin-binding and receptor-binding region. *Biochem. Biophys. Res. Commun.* **185**: 1098–1107
- 57 Eriksson A., Cousens L., Weaver L. and Matthews B. (1991) Three-dimensional structure of human fibroblast growth factor. *Proc. Natl. Acad. Sci. USA* **88**: 3441–3445
- 58 Plotnikov A. N., Schlessinger J., Hubbard S. R. and Mohammadi M. (1999) Structural basis for FGF receptor dimerization and activation. *Cell* **98**: 641–650
- 59 Reiland J. and Rapraeger A. C. (1993) Heparan sulfate proteoglycan and FGF receptor target basic FGF to different intracellular destinations. *J. Cell Sci.* **105**: 1085–1093
- 60 Bossard C., Laurell H., Van den Berghe L., Meunier S., Zambellato C. and Prats H. (2003) Translokain is an intracellular mediator of FGF-2 trafficking. *Nat. Cell Biol.* **5**: 433–439



To access this journal online:  
<http://www.birkhauser.ch>

---